Oil & Gas Science and Technology - Rev. IFP Energies nouvelles **74**, 5 (2019)

https://doi.org/10.2516/ogst/2018080

Available online at:
ogst.ifpenergiesnouvelles.fr

REGULAR ARTICLE OPEN ACCESS

Experimental study and numerical modeling for enhancing oil recovery from carbonate reservoirs by nanoparticle flooding

Mehrdad Sepehri[1], Babak Moradi[1,2], Abolghasem Emamzadeh[1], and Amir H. Mohammadi[3,*]

[1] Faculty of Petroleum Engineering, Islamic Azad University, Science and Research Branch, Tehran, Iran
[2] Iranian Central Oil Fields Company, Tehran, Iran
[3] Discipline of Chemical Engineering, School of Engineering, University Of KwaZulu-Natal, Howard College Campus, King George V Avenue, Durban 4041, South Africa

Received: 25 April 2018 / Accepted: 22 October 2018

Abstract. Nowadays, nanotechnology has become a very attractive subject in Enhanced Oil Recovery (EOR) researches. In the current study, a carbonate system has been selected and first the effects of nanoparticles on the rock and fluid properties have been experimentally investigated and then the simulation and numerical modeling of the nanofluid injection for enhanced oil recovery process have been studied. After nanofluid treatment, experimental results have shown wettability alteration. A two-phase flow mathematical model and a numerical simulator considering wettability alteration have been developed. The numerical simulation results show that wettability alteration from oil-wet to water-wet due to presence of nanoparticles can lead to 8–10% increase in recovery factor in comparison with normal water flooding. Different sensitivity analyses and injection scenarios have been considered and assessed. Using numerical modeling, wettability alteration process and formation damage caused by entrainment and entrapment of nanoparticles in porous media have been proved. Finally, the net rate of nanoparticles' loss in porous media has been investigated.

Nomenclature

a_w	Constant represents the pore size distribution index for imbibition
a_o	Constant represents the pore size distribution index for drainage
B_l	Volume factor of fluid of phase l
$C_{i,l}$	Volume concentration of nanoparticle in interval i in phase l, cm^3 cm^{-3}
C_w	Constant represents the entry pressure for imbibition
C_o	Constant represents the entry pressure for drainage
d	Diameter of nanoparticle, cm
$D_{i,l}$	Dispersion coefficient of nanoparticle in interval i in phase l, cm^2 s^{-1}
f	Flow efficiency factor
K	Absolute permeability of porous media, cm^2
K_r	Relative permeability before nanoparticle treatment
K_{rlmax}	Maximum relative permeability of phase l
K_f	Constant for fluid seepage allowed by the puggled pores
K_r'	Relative permeability after nanoparticle treatment
n	Coefficient for the relation between porosity and permeability
n_l	Exponent for phase l relative permeability
P_l	Pressure of phase l, atm
P_c	Capillary Pressure, atm
PV	Pore Volume of injection
q_l	Injection rate or production rate, cm^3 s^{-1}
r	Radii of the pores
$R_{i,l}$	Net loss rate of nanoparticle in interval i in phase l, cm^3 cm^{-3} s^{-1}
S_l	Saturation of phase l
S_{lr}	Residual saturation of phase l
S_{wc}	Connate water saturation
S^*	Normalized saturation
s_i	Surface area for nanoparticles in contact with fluids per unit bulk volume in interval i, cm^2 cm^{-3}

* Corresponding author: amir_h_mohammadi@yahoo.com

S Total surface area for nanoparticles in contact with fluids per unit bulk volume, $cm^2\ cm^{-3}$
S_v Specific area of core sample, $cm^2\ cm^{-3}$
t Time, s
u_l Flow velocity for liquid phase in porous media, $cm\ s^{-1}$
u_{lc} Critical velocity for liquid phase, $cm\ s^{-1}$
x Distance, cm
α Rate constant, cm^{-1}
β Surface area coefficient
φ Porosity of porous media
μ Viscosity of fluid, cp
$v_{i,l}$ Volume of nanoparticles available on pore surfaces per unit bulk volume of the porous media, $cm^3\ cm^{-3}$
$v_{i,l}^*$ Volume of nanoparticles entrapped in pore throats per unit bulk volume of the porous media, $cm^3\ cm^{-3}$
θ Wetting angle
σ Interfacial tension between wetting and non-wetting phase, N/m
ω Coefficient for calculating specific area

Subscripts

0 Initial value
d Deposition
e Entrapment
pt Pore throat
o Oil
w Water

1 Introduction

As regards about half of the world's known petroleum reserves exist in carbonate reservoirs, it is very important to find out how more oil can be produced from these kinds of reservoirs (Schlumberger Market Analysis, 2007). It is patently obvious that wetting property of the oil reservoirs is a highly determinant parameter for multiphase flow in porous media as well as production mechanisms. Due to this importance many of the past literature illustrate the wettability and its effect on oil recovery (Cuiec, 1990; Morrow, 1990; Ogolo *et al.*, 2012; Onyekonwu and Ogolo, 2010; Vatanparast *et al.*, 2011). Water flooding is performed as a cheap method to improve oil recovery after the primary production period (Standnes and Austad, 2000). Most of the carbonate rocks have porosities of about 5–15% and their permeabilities are influenced by connected pores which are related to pore size, shape, and arrangement (Archie, 1952; North, 1985); they have initially some degree of the oil-wet condition, therefore it is well known that the oil recovery by water flooding might have had a low ultimate oil recovery (Anderson, 1986; Buckley *et al.*, 1998). It can be deduced that the desired rock wettability is one of the key factors for a successful incremental oil recovery process. In addition, Interfacial Tension (IFT) became a very attractive parameter for oil industry researchers in the past years (Abrams, 1975; Baez *et al.*, 2012; Wagner and Leach, 1966). It has been shown that capillary force reduction through reduction in interfacial tension can significantly affect the amount of residual oil saturation in pore spaces (Abrams, 1975). Adding chemicals to injection fluids can modify rock wettability and keep the interfacial tension in desired values (Ju and Fan, 2009). Consequently, it can be expected that chemical additives may have some positive effects on water flooding process and oil recovery from carbonate rocks (Miranda *et al.*, 2012; Onyekonwu and Ogolo, 2010; Puntervold *et al.*, 2007). In the last decade, researchers working on the chemical Enhanced Oil Recovery (EOR), all tried to answer a key question that is "How the chemicals can affect the EOR processes?" (Høgnesen *et al.*, 2004; Kanj *et al.*, 2009; Mohan *et al.*, 2011; Moradi *et al.*, 2015, 2016; Ogolo *et al.*, 2012; Qiu and Mamora, 2010; Skauge *et al.*, 2010; Standnes and Austad, 2003; Tabrizy *et al.*, 2011; Wang *et al.*, 2010). Adding nanoparticles at low volume concentrations to displace water makes nanofluids. The main properties of the nanofluids strongly depend on the nanoparticles' features (Romanovsky and Makshina, 2004). The individual features of nanoparticles have attracted the attention of many researchers in the recent years (Ghosn *et al.*, 2017; Ju *et al.*, 2002, 2006; Kanj *et al.*, 2009; Kashefi *et al.*, 2018; Mandal *et al.*, 2012; Roustaei and Bagherzadeh, 2015; Sepehrinia, 2017; Wang *et al.*, 2010; Yu *et al.*, 2010). Silica nanoparticles (SiO_2) have shown a very effective role for increasing oil recovery goals (Ju and Fan, 2009; Metin *et al.*, 2013; Moradi *et al.*, 2015, 2016). Many researchers have studied the potential of silica nanoparticles for EOR objectives in sandstone rocks, with experimental and/or simulation approaches (El-Amin *et al.*, 2012, 2013; Hendraningrat and Shidong, 2012; Hendraningrat *et al.*, 2013; Ju and Fan, 2009; Ju *et al.*, 2002, 2006, 2012; Metin *et al.*, 2013; Onyekonwu and Ogolo, 2010; Parvazdavani *et al.*, 2012; Roustaei *et al.*, 2012; Shahrabadi *et al.*, 2012; Yu *et al.*, 2012). Many papers report the experimental effects of these nanoparticles on EOR parameters for carbonate rocks (Al-Anssari *et al.*, 2016, 2018; Kanj *et al.*, 2009; Karimi *et al.*, 2012; Maghzi *et al.*, 2011; Metin *et al.*, 2013; Moradi *et al.*, 2015, 2016; Roustaei and Bagherzadeh, 2015; Sun *et al.*, 2017; Yu *et al.*, 2012); But, there are no studies on the simulation and mathematical modeling of the effects of silica nanoparticles on the production parameters as an additive in water flooding for carbonate rocks. In the current study, several core flooding with and without adding nanoparticles to injection fluid have been implemented and the effects of these nanoparticles on contact angle and interfacial tension are discussed (used cores were taken from one of the carbonate oil reservoirs in the south of Iran). We prove the effects of silica nanoparticles on enhancing oil recovery from an oil-wet carbonate system by a precise numerical model (interfacial tension reduction because of nanoparticle treatment has been discarded in our model). We have performed several sensitivity analyses on different properties such as nanofluid's concentrations and injection volume. In addition, different injection scenarios have been considered in our model.

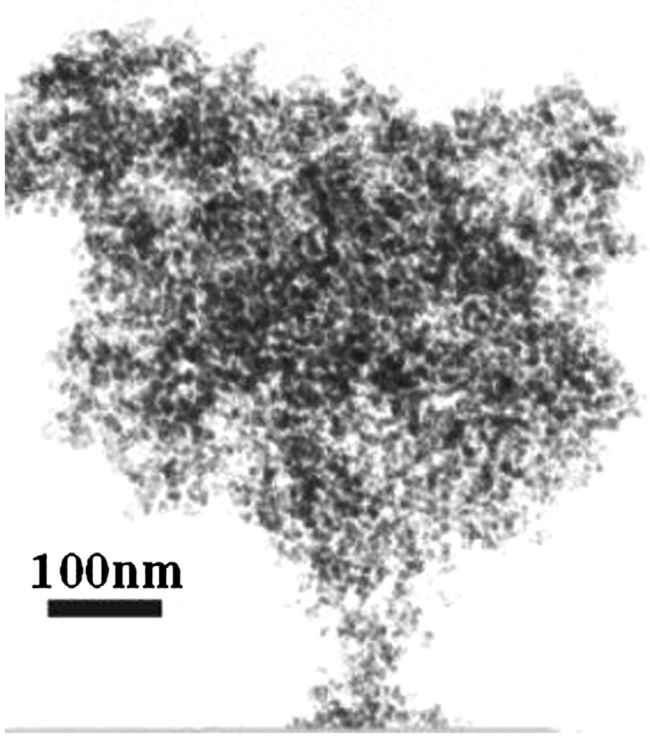

Fig. 1. SEM image of SiO_2 nanopowder (www.us-nano.com).

2 Core flooding experiments

2.1 Physical properties of silica nanoparticles

In this study, the commercial silica nanoparticles were used that their diameters are in the range of 20–70 nm. Figure 1 shows the SEM image of used nanoparticle as well as in Figure 2, we have shown that the particles' sizes have a normal distribution. The basic information of the used nanoparticles is reported in Table 1.

2.2 Physical properties of carbonate rock

Experimental studies show that the porosity and permeability of the employed core samples are about 15% and 16 md, respectively. As well as all of these samples are non-fractured. Table 2 gives the main properties of carbonate rock samples that they were used in our experiments.

Several core flooding experiments were performed to check the capability of the nanofluids for enhancing oil recovery. These experiments were done under various conditions such as different injection rate, different water/nanofluid injection scenarios and different inlet concentration of nanofluids. We performed all experiments at an initial pressure equal to 100 psi and the fixed temperature was 25 °C. Figure 3 shows the schematic diagram of the flooding apparatus which mainly consists of core holder, pressure meter, back pressure regulator, valves and controllers and pumps. The maximum possible core diameter and length for the used core holder are 3.75 cm and 40 cm, respectively. The confining pressure for the mentioned core holder must be at least 400 psi upper than core pressure; in this case the confining pressure was 600 psi.

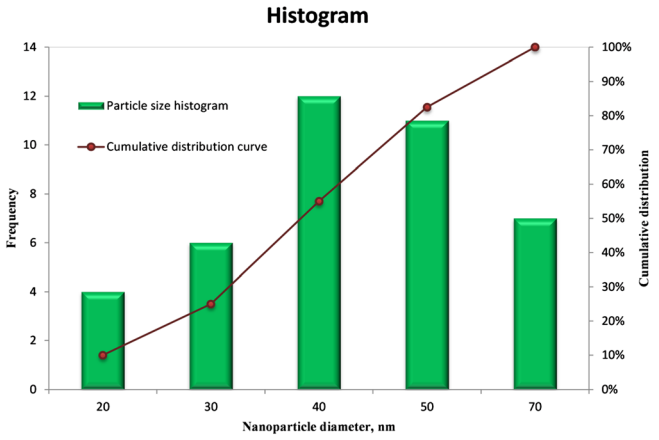

Fig. 2. Particle size distribution curve.

Table 1. Physical properties of commercial silica nanoparticles.

Parameter	Unit	Value
Particle size, nm	nm	20–70
Wettability	–	Hydrophilic
Color	–	White
Purify	%	>99.5
Dispersed in	–	Water
Bulk density	g/cc	≈0.10
True density	g/cc	≈2.40
Specific Surface Area (SSA)	m^2/g	160–600

Table 2. Used carbonate rock properties.

Parameter	Unit	Value
Sample name	–	C26-W2
Location	–	South of Iran
Structure	–	Non-fractured
Depth of core	m	2730
Length of core	cm	10
Cross section area of core	cm^2	8.6
Rock density	g/cc	2.56
Porosity	%	15
Permeability	md	16

2.3 Experimental procedure

First, the cylindrical shape core was cleaned and dried with an ultrasonic bath and an oven, respectively. The dried core was used to determine the porosity and absolute

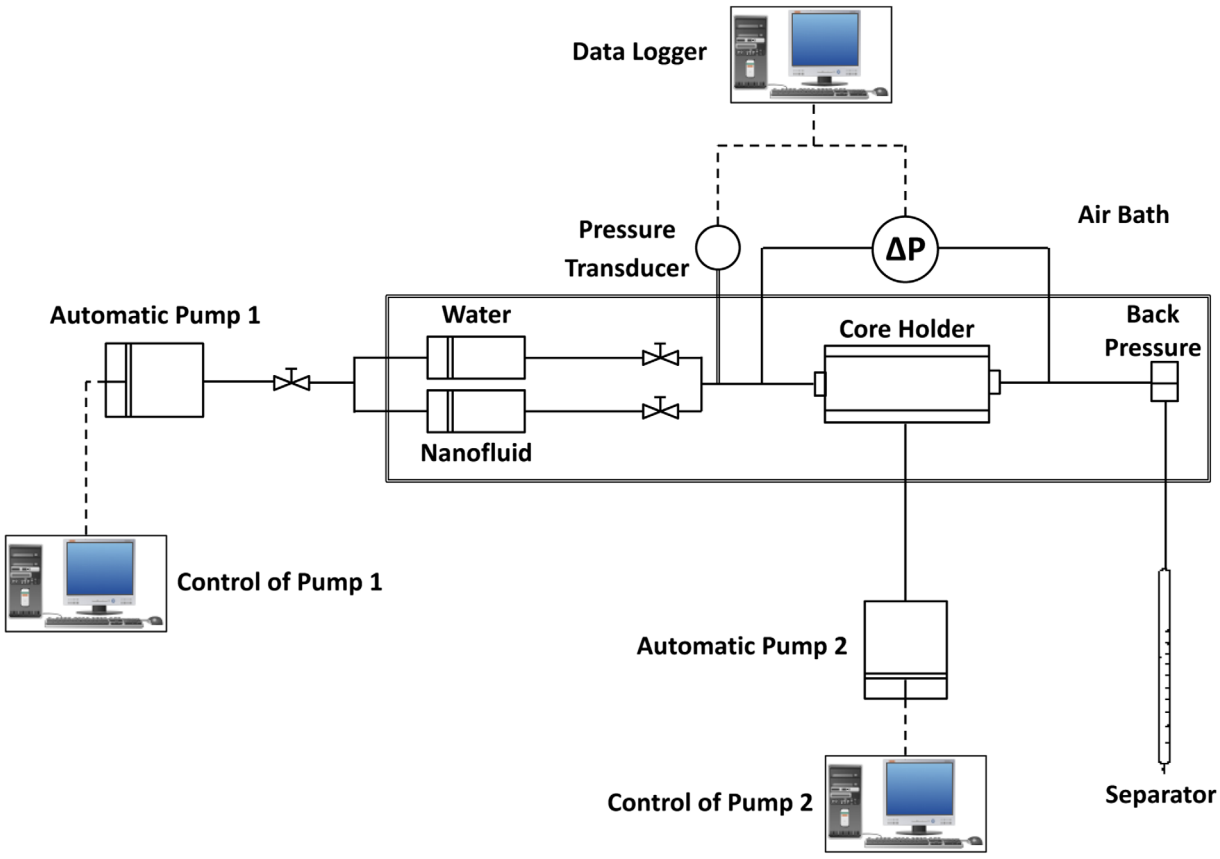

Fig. 3. Schematic diagram of core flooding apparatus.

permeability of the rock. Then, saturation process was applied on core to saturate it with brine. The saturated core was placed into a core holder to implement water flooding process. At the water flooding process the liquid permeability was measured again. After water flooding, oil was injected into core for producing water at the outlet; this process was continued until no water production occurred. Afterwards, the core took out from the core holder and placed in an oil container to implement the aging process (the aging process took 9 days). Then, the core was injected by oil in core holder to produce the remaining water of the core as a result of aging process (the aging process can make the rock oil-wet and contact angle experiment confirms it). The core was then ready for the main injection process (water and nanofluid flooding). The oil and brine properties are reported in Tables 3 and 4, respectively; and oil composition is given in Table 5.

At first, the flooding experiment was performed only with water. 6 PV of water was injected into the core and the produced oil and water from the outlet of the core were collected into a scaled container in which 35.8% of the original oil volume was produced. After that in order to repeat the flooding test under another injection rate scenario, the core was injected with oil to reach the initial condition again (irreducible water saturation condition). The flooding process was then conducted with both water and nanofluid. First, 1 PV of water was injected, then 1 PV of nanofluid was injected which followed by injection of 4 PV of water; observed oil recovery was 44.9%. Figure 4 displays the experimental results of core flooding with and without nanoflooding.

Table 3. Properties of oil sample.

Parameter	Unit	Value
API of oil	°API	27.30
Specific gravity of oil – 15.56/15.56 °C	–	0.8911
Density @ 15.56 °C – 0.1 MPa	g/cc	0.89
Viscosity @ 15.56 °C – 0.1 MPa	cp	30.3
Molecular weight of reservoir oil	g/gmol	102
Molecular weight of remaining oil	g/gmol	220
Molecular weight of C_{12}^{+}	g/gmol	310
Specific gravity of C_{12}^{+}	–	0.9287

Table 4. Properties of brine sample.

Parameter	Unit	Value
Salinity	ppm	80 000
Density @ 15.56 °C – 0.1 MPa	g/cc	1.024
Viscosity @ 15.56 °C – 0.1 MPa	cp	0.7

Table 5. Crude oil composition.

Composition	Mole percent (%)
H_2S	0
N_2	0
CO_2	0
C_1	0
C_2	0.07
C_3	0.45
iC_4	0.53
nC_4	1.4
iC_5	0.61
nC_5	0.52
C_6	9.12
C_7	7.25
C_8	7.13
C_9	6.12
C_{10}	6.10
C_{11}	5.03
C_{12+}	55.67
Total	100

3 Describing the nanoparticle transportation in porous medium using mathematical modeling

3.1 Assumptions

The following assumptions are considered in the current model:

- One-dimensional flow under isothermal condition.
- Compressible rock and fluids.
- Heterogeneous porous media.
- The Darcy's law governs the fluid flow in porous media.
- The gravity force is neglected.
- The viscosity and density of the fluids are various with pressure.
- Both oil and water are Newtonian fluids.

3.2 Fluid transportation in porous media

It is known that the fluid flow in porous medium follows Darcy's law and the governing equation for Newtonian fluids as well as a slightly compressible multiphase flow are as follows (Ju *et al.*, 2012):

$$\mathrm{div}\left(\frac{K\cdot K_{rl}}{B_l\cdot\mu_l}\mathrm{grad}(P_l)\right)+q_l=\frac{\partial}{\partial t}(\varphi.S_l/B_l), \qquad (1)$$

where t is time, φ is the porosity of porous media, S, μ and P are saturation, viscosity and pressure of fluids, respectively, K is absolute permeability, K_r is relative permeability, B is the volume factor of fluid, q is the production or injection rate of fluid, and subscript l refers to oil and water phases. For saturated flow of the oil and water phases, the sum of saturations of oil and water is equal to 1 (Ju *et al.*, 2012):

$$S_w+S_o=1. \qquad (2)$$

3.3 Mixed-wet capillary pressure

Injecting the water-nanoparticles suspension into an oil reservoir can change the wettability of the porous media from oil-wet to water-wet; therefore, we are allowed to consider the rock wetness as a mixed-wet condition. Skjaeveland *et al.* introduced a capillary pressure equation for mixed-wet systems at primary drainage condition, based on Brooks and Corey equation (Skjaeveland *et al.*, 1998). Other conditions between strong water-wet and strong oil-wet limits should be considered. Therefore, El-Amin *et al.* generated a general equation for any conditions between the two mentioned above limitations (El-Amin *et al.*, 2013). It is expressed as:

$$P_c=C_{\mathrm{w}}\left(\frac{S_w-S_{wr}}{1-S_{wr}}\right)^{-a_w}+C_o\left(\frac{S_o-S_{or}}{1-S_{or}}\right)^{-a_o}, \qquad (3)$$

where C_w and C_o are constants representing the entry pressure for imbibition and drainage, respectively. The constants $1/a_w$ and $1/a_o$ are the pore size distribution indices for imbibition and drainage, respectively. Both S_{wr} and S_{or} are residual saturations for water and oil phases, respectively (El-Amin *et al.*, 2013).

3.4 Calculation of relative permeability

A modified Brooks-Corey's correlation is used to consider relative permeabilities of phases for a two phase flow which is defined by a Power-Law function as follows (Ahmed, 2006):

$$K_{rw}=K_{rw\max}S^{*n_w}, \qquad (4)$$

$$K_{ro}=K_{ro\,max}(1-S^*)^{n_o}, \qquad (5)$$

$$S^*=\frac{(S_w-S_{wc})}{(1-S_{wc}-S_{or})}, \qquad (6)$$

where K_{rwmax}, n_{w}, K_{romax} and n_o are the maximum relative permeability and exponents of the water and oil relative permeabilities, respectively. The S_{wc} and S_{or} are saturation of connate water and residual oil, respectively (Ahmed, 2006).

3.5 Nanoparticles transportation in porous medium

Because of the nanoparticles' surface charge, some sort of nanoparticles can exist in water phase and the other ones can exist in oil phase. Since the nanoparticles' sizes are ranging from 20 to 70 nm, we should consider Brownian diffusion. Therefore, the nanoparticles transport in porous media is

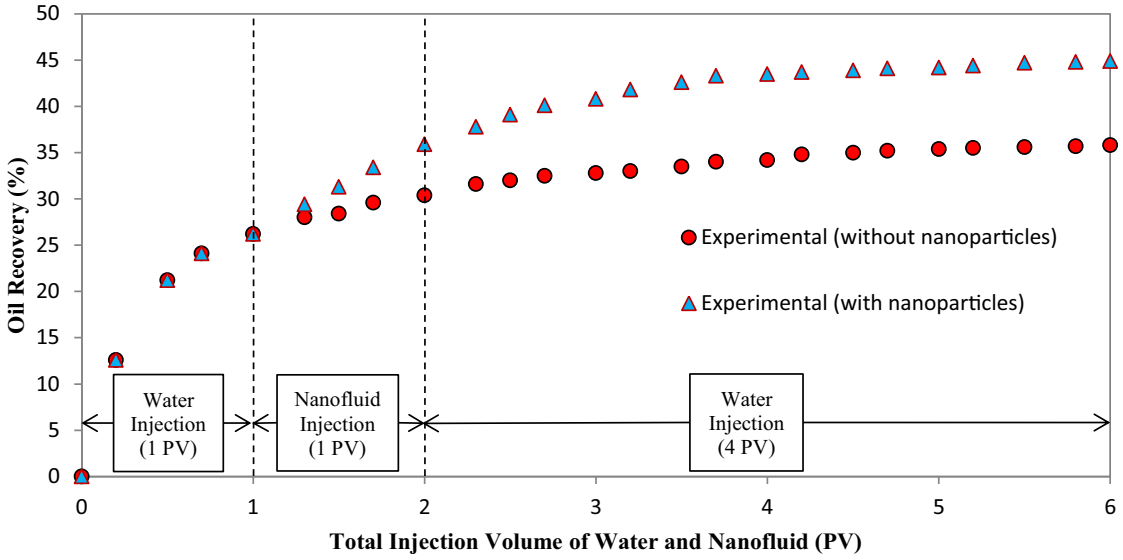

Fig. 4. Experimental results of flooding process.

defined as the following governing equation (Ju and Fan, 2009):

$$u_l \frac{\partial C_{i,l}}{\partial x} + \varphi S_l \frac{\partial C_{i,l}}{\partial t} - \frac{\partial}{\partial x}\left(\varphi S_l D_{i,l} \frac{\partial C_{i,l}}{\partial x}\right) + R_{i,l} = 0, \quad (7)$$

where $i = 1, 2, \ldots n$.

The initial and boundary conditions, for the above equation are expressed as:

$$C_{i,l} = 0 \,@\, t = 0,$$

$$C_{i,l} = C_{i,l,in} \,@\, x = 0,$$

where $C_{i,l}$ is the volume concentration of nanoparticles in interval i in phase l, $D_{i,l}$ is the dispersion coefficient of nanoparticles in interval i in phase l, $R_{i,l}$ is the net rate of loss of nanoparticles in interval i in phase l, and $C_{i,l,in}$ is the concentration of the interval i of nanoparticles in the injected fluids (Ju and Fan, 2009).

3.6 Net loss rate of nanoparticles in transport process

As a whole, for a non-fractured carbonate rock, pore surfaces and throats are the most important factors to fine particles transportation. Generally, two types of nanoparticles retention in porous medium can occur during nanoparticles transportation: deposition on pore surfaces and blockage in pore throats (Ju *et al.*, 2012). The retained nanoparticles can be desorbed by hydrodynamic forces, and then possibly adsorb or get entrapped, respectively on other sites of the pore and at other pore throats (Ju *et al.* 2012). By modifying the Ju's model (Ju *et al.* 2002), $R_{i,l}$ in equation (7) is given by:

$$R_{i,l} = \frac{\partial v_{i,l}}{\partial t} + \frac{\partial v^*_{i,l}}{\partial t}, \quad (8)$$

where $v_{i,l}$ is the volume of nanoparticles of the interval i in contact with phase l available on the pore surfaces per unit bulk volume of carbonate rock, $v^*_{i,l}$ is the volume of nanoparticles of the interval i in contact with phase l entrapped in pore throats per unit bulk volume of carbonate rock due to plugging and bridging (Ju *et al.*, 2012).

Flow velocity has an upper limit called critical velocity; below the critical velocity only particle retention can occur while above that velocity both retention and entrainment may occur simultaneously (Gruesbeck and Collins, 1982). A modified Gruesbeck and Collins's model for the surface deposition can be written as (Ju *et al.*, 2002):

$$\frac{\partial v_{i,l}}{\partial t} = \begin{cases} \alpha_{d,i,l} u_l C_{i,l} & u_l < u_{lc} \\ \alpha_{d,i,l} u_l C_{i,l} - \alpha_{e,i,l} v_{i,l} (u_l - u_{lc}) & u_l > u_{lc} \end{cases}. \quad (9)$$

The initial condition for equation (9) is:

$$v_{i,l} = 0 \,@\, t = 0.$$

In equation (9), $\alpha_{d,i,l}$ and $\alpha_{e,i,l}$ are rate coefficients for surface retention and entrainment of nanoparticles in interval i in the phase l, respectively, and u_{lc} is the critical velocity for the phase l to entrain particles (Ju *et al.*, 2012).

The rate equation for the entrapment of the particles in pore throats in interval i in the phase l is expressed by (Ju *et al.*, 2002):

$$\frac{\partial v^*_{i,l}}{\partial t} = \alpha_{pt,i,l} u_l C_{i,l}, \quad (10)$$

where $\alpha_{pt,i,l}$ is a constant for pore throat blocking. The initial condition for equation (10) is (Ju *et al.* 2012):

$$v^*_{i,l} = 0 \,@\, t = 0.$$

3.7 Porosity and absolute permeability changes

In presence of nanoparticles, both deposition on the pore surfaces and blocking in pore throats can reduce the

porosity and absolute permeability. The local and instantaneous porosity is expressed by (Ju *et al.*, 2002):

$$\varphi = \left(\varphi_0 - \sum \Delta\varphi\right), \tag{11}$$

where $\sum \Delta\varphi$ denotes the porosity changes by release and retention of nanoparticles in the porous medium which is expressed by the following equation (Ju *et al.*, 2002):

$$\sum \Delta\varphi = v_{i,l} + v^*_{i,l}. \tag{12}$$

The expression for the local and instantaneous permeability due to the deposition and blocking of particles is obtained by (Ju *et al.*, 2002):

$$K = K_0\left[(1-f)k_f + f\varphi/\varphi_0\right]^n, \tag{13}$$

where K_0 and φ_0 are initial permeability and porosity, K and φ are instantaneous local permeability and porosity of the porous media, k_f is a fluid seepage constant which is related to plugged pores, and f is the fraction of the original cross-sectional area open to flow (Ju *et al.*, 2012).

3.8 Capillary pressure affected by nanoparticles

As a result of presence of nanoparticles in fluid, the capillary force can be changed due to interfacial tension alteration, which will affect the multiphase flow behavior (Løvoll *et al.*, 2005). Capillary pressure for a two phase system for an ideal thin tube with equal diameters is expressed by the following equation (Ju *et al.*, 2012):

$$P_c = \frac{2\sigma\cos\theta}{r}, \tag{14}$$

where σ is the interfacial tension between wetting and non-wetting phases N/m; θ is the wetting angle; and r is the radius of the capillary (Ju *et al.*, 2012).

Because of the existence of nanoparticles in the fluid during the treatment process, two kinds of alteration between fluids and rock surface can occur: changing interfacial tension and changing contact angle. Then, the interfacial tension can be considered as a function of the nanoparticles concentration in the fluid and contact angle. The capillary pressure, in porous medium, is obtained by mercury injection experiments and it is considered as a function of the wetting phase saturation if wettability does not change. By changing the wettability resulted by nanoparticles treatment and the carbonate rocks' heterogeneity, the capillary pressure can be considered as the below conception (Ju *et al.*, 2012):

$$P_c = f\left(S_w, C_l, v_l + v^*_l\right). \tag{15}$$

3.9 Evaluating the relative permeability affected by nanoparticles

The wettability of pore surfaces is the most important factor to determine the relative permeability of a porous media. As it was mentioned earlier, the nanoparticles retention in porous media can change the wettability of the pore surfaces and the relative permeability curves can be shifted (Ju *et al.*, 2012).

Assuming a point contact touching of spherical particles and using the real volume of particles as the denominator, the specific area of the particles is $6/d$; where d is the diameter of the particles (Qin and Li, 2001).

The adhered nanoparticles to the pore walls, first spread as a single layer, the surface area for particles in interval i is given by the following equation (Ju *et al.*, 2002):

$$s_i = \left(v_{i,l} + v^*_{i,l}\right) s_{bi} = \left(v_{i,l} + v^*_{i,l}\right)\frac{6}{d_i}. \tag{16}$$

The total surface area which is in contact with fluids for all intervals per unit bulk volume of the porous media is calculated by (Ju *et al.*, 2002):

$$s = \beta \sum_{i=1,\, l=w,o}^{n} \left(v_{i,l} + v^*_{i,l}\right)\frac{6}{d_i}, \tag{17}$$

where β is the surface area coefficient. An equation for calculating the specific area which is given by Qin and Li (2001), was modified herein, which is expressed by (Ju *et al.*, 2002):

$$s_v = 7000\varphi\sqrt{\frac{\varphi}{\omega K}}, \tag{18}$$

where ω is a coefficient for calculating specific area. We assume that the relative permeabilities of water and oil phases are, respectively, K_{rwj} and K_{roj} at a water saturation, S_{wj} before nanoparticles treatment (Ju *et al.*, 2012). When the surfaces per unit bulk volume of the porous media are fully covered by nanoparticles, the relative permeabilities of water and oil phases are taken as K'_{rwj} and K'_{roj}, respectively. The water and oil relative permeability are assumed to be a linear function of the surfaces covered by nanoparticles, therefore, the relative permeabilities of water and oil phases are as following (Ju *et al.*, 2002):

$$K'_{rwjp} = K_{rwj} + \frac{K'_{rwj} - K_{rwj}}{s_v}s, \tag{19}$$

$$K'_{rojp} = K_{roj} + \frac{K'_{roj} - K_{roj}}{s_v}s, \tag{20}$$

when $s \geq s_v$, the total surfaces per unit bulk volume of the porous media are fully covered by nanoparticles which are adsorbed or entrapped in porous medium, therefore, the nanoparticles change the wettability properties of porous media ($R_s = \frac{s}{s_v} = 1$) (Ju *et al.*, 2012).

4 Mathematical modeling procedure

Generally, we are faced with a nonlinear system which consists of the continuity equations of oil and water phases

(Eq. (1)), the convection-diffusion-adsorption equation (Eq. (7)), and a series of auxiliary equations (Ju and Fan, 2009). To solve the nonlinear equation system, the finite difference method can be used. In the current study, the IMPES (Implicit Pressure-Explicit Saturation) method was used to solve the pressure-saturation equation and an implicit method was applied to solve the convection-diffusion-adsorption equation to achieve maximum stability. Following procedure is used for the current modeling:

1. Obtaining the pressure and saturation distribution by solving the mass balance equation.
2. Velocity calculation through Darcy's law.
3. The nanoparticles concentration distribution in interval i is obtained by solving the convection-diffusion-adsorption equation.
4. The new porosity φ, absolute permeability K, and relative permeabilities of oil and water phases for each grid block are calculated.
5. If maximum simulation time is not reached, return to the first step.

It should be mentioned that the above procedure must be done for each time step until reaching last time step of modeling; Figure 5 shows the mathematical modeling flowchart.

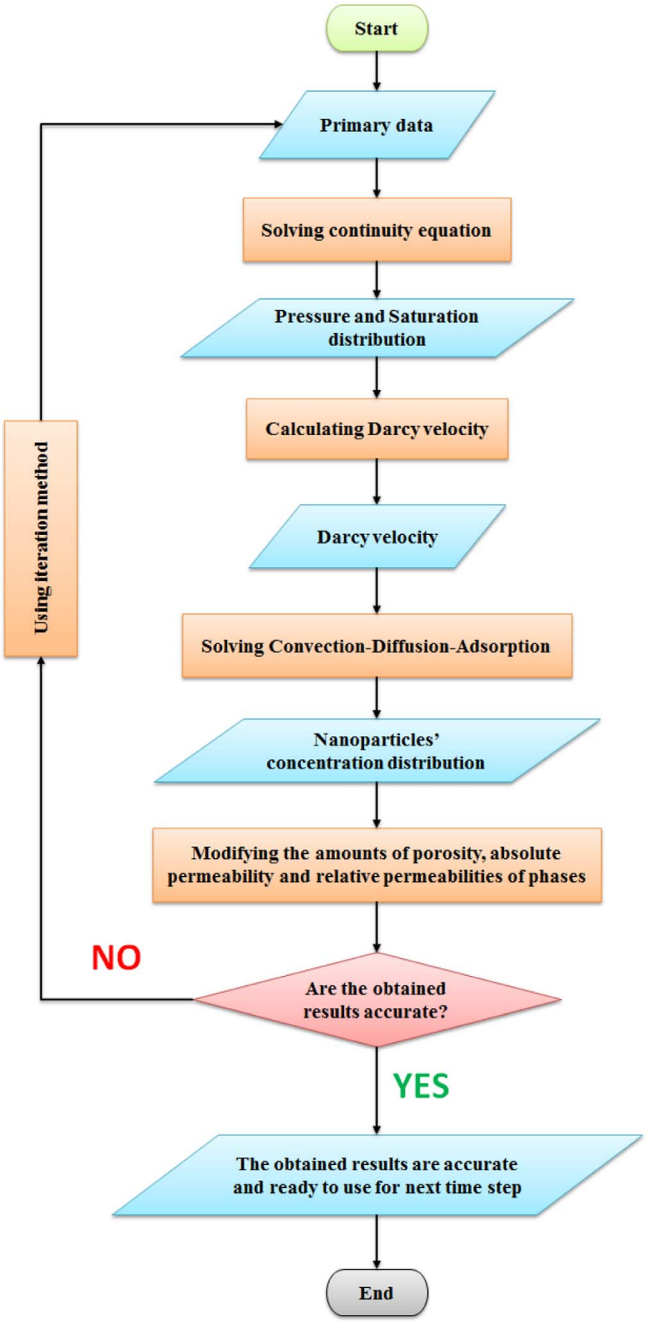

Fig. 5. Mathematical modeling flowchart.

5 Results and discussion

This section presents an instance which can be implemented for enhanced oil recovery from a non-fractured carbonate oil reservoir. Since the nanoparticles can adhere onto carbonate pore bodies therefore they cause wettability changes for pore surfaces, and they could be applied for enhanced oil recovery purposes.

5.1 Experimental observations of the physical effects on porous media due to presence of nanoparticles

The nanoparticles' sizes are in the range of 20–70 nm. On the other hand, the experimental results show that the radii of the pore throats are about 8.0×10^0 to 5.2×10^4 nm, therefore some of the particles are smaller than the pore throats as well as some of them are bigger. When the nanoparticles are transported through the porous media, some pores can be blocked due to plugging and/or bridging by the bigger nanoparticles. In addition, because of the activity of the nanoparticles, they may adhere onto pore bodies. As it is known, the surface charge of the hydrophilic silica nanoparticles and the pore surfaces' charge of the carbonate rocks are generally different. Thus, adhering the nanoparticles onto pore surfaces can lead to wettability alteration of the rocks. In this study, the contact angle measurements were performed to find out how the nanoparticles' retention in porous media can change rock wettability. Three steps of the wettability alteration process due to presence of silica nanoparticles were measured which are shown in Figure 6. As can be seen, the initial contact angle was 140.34° before any treatment (Fig. 6A). After 0.5 PV of nanofluid was injected into core plug, the contact angle of the oil drop became 98.60° (Fig. 6B) and finally after injecting 1 PV of the nanofluid, wettability alteration process was completely done and the contact angle reached to 47.53° (Fig. 6C).

Another effect of silica nanoparticles is reduction of interfacial tension between oil/water surface. The Pendant drop method was used to measure the variation of interfacial tension due to presence of nanoparticles in injected fluid. The initial interfacial tension value was 26.3 mN/m. A stepwise increasing of nanofluid concentration was

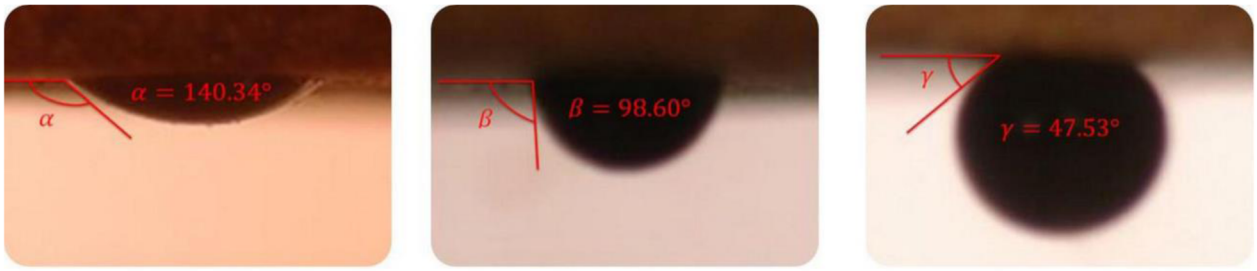

(A) Oil drop on a slice of carbonate rock sample before nanoparticle treatment.

(B) Oil drop on a slice of carbonate rock sample after 0.5 PV nano-fluid injection.

(C) Oil drop on a slice of carbonate rock sample after 1 PV nano-fluid injection.

Fig. 6. Wettability alteration due to nanofluid injection.

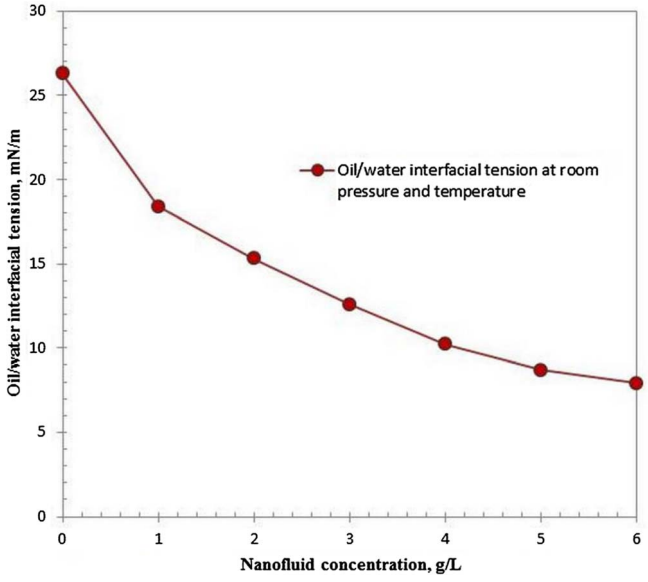

Fig. 7. Oil/water interfacial tension before and after using nanofluid.

employed to evaluate the variation of interfacial tension. Figure 7 shows that the higher concentration of injected nanofluid can lead to lower interfacial tension; the last measurement of interfacial tension was 7.9 mN/m at a concentration of 6 g/L.

5.2 Mathematical modeling results of silica nanoparticles transportation through porous media

It is obvious that in a weak water-wetting rock, the sweep efficiency of water flooding is less than a strong water-wetting rock (Ju and Fan, 2009). Since the hydrophilic nanoparticles could increase the inclination of strong water-wetness using hydrophilic nanoparticles which cover pore walls, they can be applied in field usages for EOR purposes. The current modeling example was performed to predict production performance when the hydrophilic nanoparticles are injected. The main numerical simulation's parameters are listed in Table 6.

Table 6. Parameters for simulation.

Parameter	Unit	Value
Number of grid	–	40
Grid size	cm	0.25
Cross-sectional area	cm^2	8.6
Original porosity	Fraction	0.15
Original permeability	md	16
Original saturation of oil	Fraction	0.8
Original viscosity of reservoir oil	cp	30.3
Viscosity of injection water	cp	0.7
Injection rate of water	cc min^{-1}	0.2
Pressure at the outlet boundary	psi	100

We have used nanoparticles with size 40 nm in the present model, as their properties are shown in Table 7.

Figure 8 shows the oil recovery after injection of 6 PV of brine into the core sample. The points in this figure represent the experimental data that were obtained from core flooding experiments in the laboratory and the continuous line indicates the numerical results. As it is known, the numerical error is less than 1%, so the proposed model can efficiently simulate the core flooding process before nanofluid injection.

We implemented the nanofluid injection under three different scenarios as they are shown in Table 8.

Figure 9 presents the oil recovery after 6 PV injection of water and nanofluid (NP40) under second scenario's condition. At first, 1 PV of water was injected, then 1 PV of nanofluid (at the inlet concentration of 0.02 cc/cc) was injected followed by 4 PV of brine injection. The points that can be seen in Figure 9 were obtained from experimental works and the continuous line is based on the numerical results. As regards the numerical error is less than 1% with respect to experimental data, we can conclude that the current proposed model is highly reasonable to simulate the nanofluid injection process for enhanced oil recovery.

Figure 10 shows the effects of concentration of nanoparticles (NP40) on oil recovery under second scenario injection's condition. It gives that, the higher concentration

Table 7. Parameters of nanoparticles used for numerical simulation.*

NP Indicator	Diameter of NP (nm)	$\alpha_{d,i,l}$ (cm^{-1})	$\alpha_{e,i,l}$ (cm^{-1})	$\alpha_{pt,i,l}$ (cm^{-1})	$D_{i,l}$ ($cm^2\ s^{-1}$)	u_{lc} ($cm\ s^{-1}$)
NP40	40	0.18	0.35	0.0162	0.00051	0.00049

*NP denotes the nanoparticle.

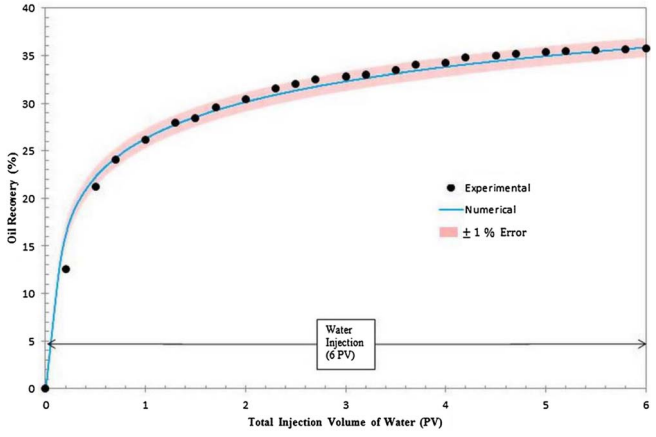

Fig. 8. Experimental data and numerical results matching (before nanofluid treatment).

Table 8. Different injection scenarios.*

	1st PV	2nd PV	3rd PV	4th PV	5th PV	6th PV
1st scenario	W	N	W	N	W	W
2nd scenario	W	N	W	W	W	W
3rd scenario	N	N	N	N	N	N

*W and N denote the Water injection and Nanofluid injection, respectively.

of injected nanoparticles can lead to increase the oil recovery. As can be seen, when the concentration increases from 0.02 to 0.04, the ultimate oil recoveries are very close together, therefore, if the concentration of nanoparticles' slug be larger than 0.02, it does not have a significant effect on oil recovery. After 1 PV of water was injected, the oil recovery reached to 26.27%. It is recognized that at the start of nanofluid injection, no obvious immediately oil recovery improvement can be seen. It shows the ultimate oil recovery is from 35.84% (nanoparticle concentration = 0.0) to 45.36% (nanoparticle concentration = 0.04). The oil recovery reached to 45.23% for nanoparticle concentration of 0.02 and the incremental oil recovery is 9.39% compared with usual water injection. It points that when the concentration of injected nanofluid is less than 0.02, the increase in oil recovery can be significant due to nanoparticle concentration increase. It indicates that, in this case, injection of 1.0 PV of nanofluid with the concentration of 0.02 can lead to the fully covered pore surfaces by adsorbed nanoparticles. More than enough nanoparticle adsorption on pore bodies does not cause any further change to the pore surfaces' wettability, so that, the increase in concentration above 0.02 cannot lead to an obvious higher oil recovery. In addition, multilayer adsorption of nanoparticles on pore bodies may lead to intensive formation damage (porosity and permeability reduction). The ultimate recovery values (after the end of 6 PV fluid injection) are shown in Table 9.

Figure 11 gives the water cut (volume fraction of water in produced fluid) changing throughout production and injection time. The water cut of produced fluid was zero before 0.11 PV water was injected and after the water breakthrough at the outlet, then water cut increases considerably. After 1.0 PV of water was injected, the water cut increased to 95.39%. Because of the behavior of two-phase flow at the outlet which affects the amount of water cut, the water-cut does not have a sudden decrease until the nanofluid changes the rock's wettability to a lower tendency of water-wetting. Therefore, the injected nanofluid can lead to water cut decreasing and this process should be more intensed for nanofluid injection at higher concentration. Water cut decreased to 84.31% after injection 0.45 PV of nanofluid (with the concentration of 0.04 and under second scenario injection's condition). Table 10 gives the minimum values of the water cut after nanofluid injection.

Figures 12 and 13 show the results of sensitivity analysis on different injection scenarios at high nanoparticle concentration (nanoparticle concentration = 0.02). At high concentrations, because of the higher rate of loss, wettability alteration process from oil-wetting to water-wetting done at earlier injected pore volumes. As can be seen in Table 8, in third scenario, nanofluid is injected at the beginning of the flooding process, therefore the deviation from first and second scenarios (Figs. 12 and 13) are patently obvious. In the first and second scenarios, flooding process starts with 1.0 PV of injected water followed by injection of 1.0 PV of nanofluid and as regards, injecting of 1.0 PV of nanofluid with the concentration of 0.02 can lead to the fully covered pore surfaces by adsorbed nanoparticles (refer to Fig. 10), therefore, an additional injected nanofluid in the first scenario does not have any further effects on oil recovery, so the first and second scenario's curves are completely matching.

Figures 14 and 15 give the results of sensitivity analysis on different injection scenarios at low nanoparticle concentration (nanoparticle concentration = 0.005). As can be seen, for third scenario, because the nanofluid is injected thorough the injection process, it causes maximum effects on the rock and fluid properties and consequently it

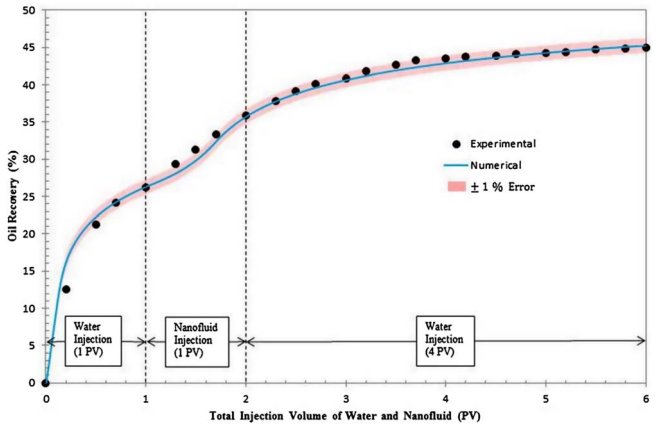

Fig. 9. Experimental data and numerical results matching (after nanofluid treatment).

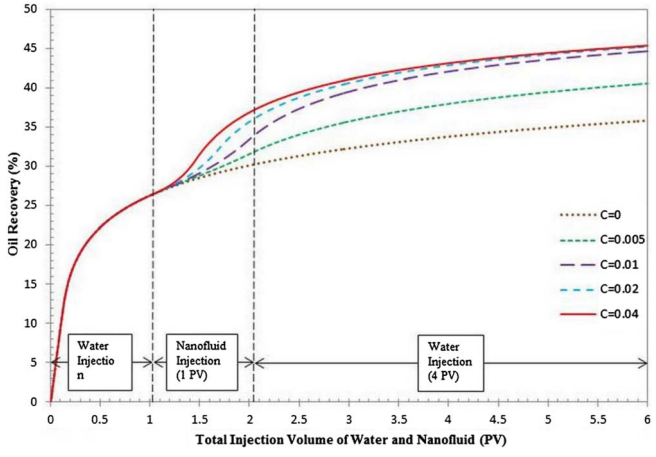

Fig. 10. The relations between oil recovery and the concentration of nanofluid.

Table 9. Ultimate recovery factor after injection of 6 PV fluid (at different nanofluid concentration).

Concentration (cc/cc)	Ultimate recovery factor (%)
0	35.84
0.005	40.57
0.01	44.65
0.02	45.23
0.04	45.36

causes maximum oil recovery and minimum water cut. In the first and second scenarios, injection process starts with 1 PV of water and then 1 PV of nanofluid, therefore both first and second scenarios' curve for the first two PV of injected fluids are completely overlapped. In the second scenario, an injected PV of nanofluid is followed by 4 PV of brine, but for the first one after re-injection of 1 PV of

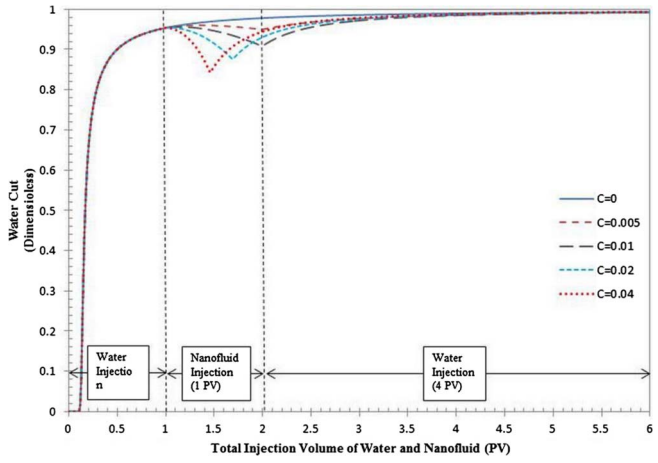

Fig. 11. The relations between water cut and the concentration of nanofluid.

Table 10. Minimum water cut after injecting 1 PV of nanofluid (at different concentration).

Concentration (cc/cc)	Minimum water cut (%)
0.005	94.97
0.01	90.81
0.02	87.55
0.04	84.31

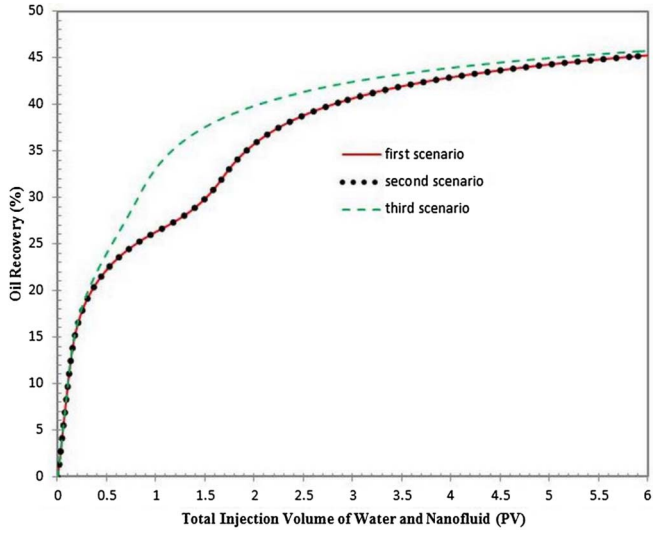

Fig. 12. The effect of different injection scenarios on oil recovery at high nanoparticle concentration (0.02).

water, 1 PV of nanofluid is injected and finally injection of 2 PV of water. In general, for the first, second, and third scenarios we have 2, 1, and 6 PV of injected nanofluid, respectively. As a result, for the nanofluid with

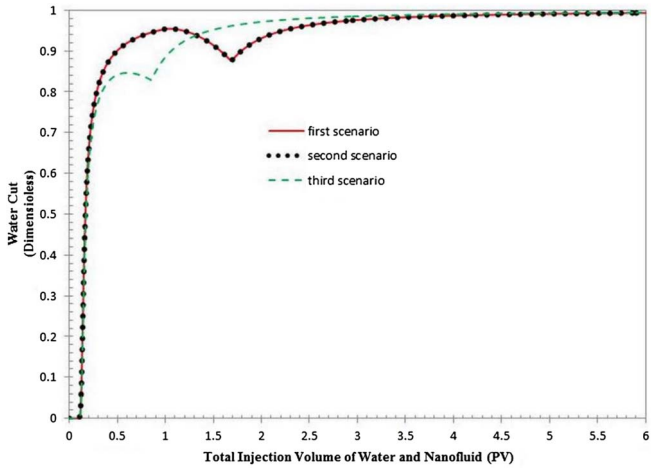

Fig. 13. The effect of different injection scenarios on water cut at high nanoparticle concentration (0.02).

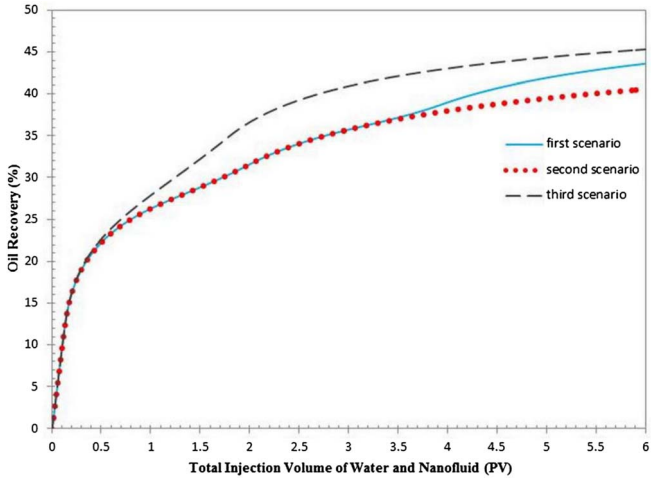

Fig. 14. The effect of different injection scenarios on oil recovery at low nanoparticle concentration (0.005).

low concentrations, since the loss rate of nanoparticles is low, the first layer of adsorbed nanoparticles on pore bodies is formed in the longer time; therefore wettability alteration process is done gradually. As can be seen, in low nanoparticles' concentration, injecting more PV of nanofluid results in increasing the oil recovery and decreasing the water cut.

Figures 16–19 show the normalized porosity and permeability profiles for different PV (Figs. 16 and 17) and different inlet concentration (Figs. 18 and 19) of injected nanofluid. Increasing the injected PV or inlet concentration, at the proximity of inlet, the normalized porosity and permeability are smaller than those at the proximity of outlet. The decrease in porosity and permeability results from nanoparticles' retention on pore surfaces and entrapment in pore throats.

Figures 20 and 21 give the wettability alteration process for different PV and inlet concentration of injected

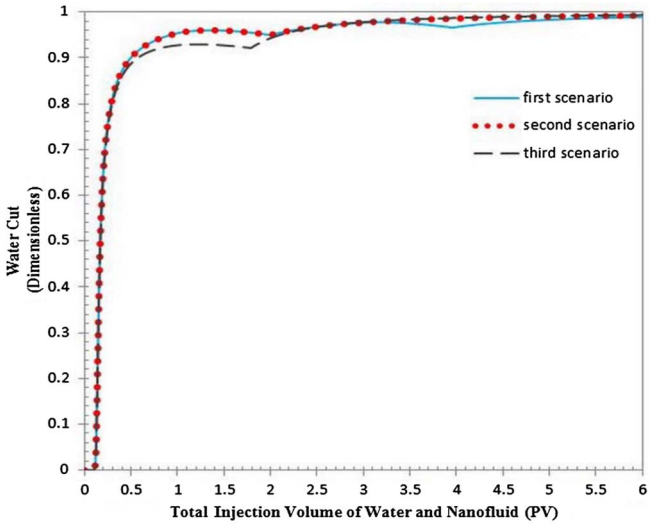

Fig. 15. The effect of different injection scenarios on water cut at low nanoparticle concentration (0.005).

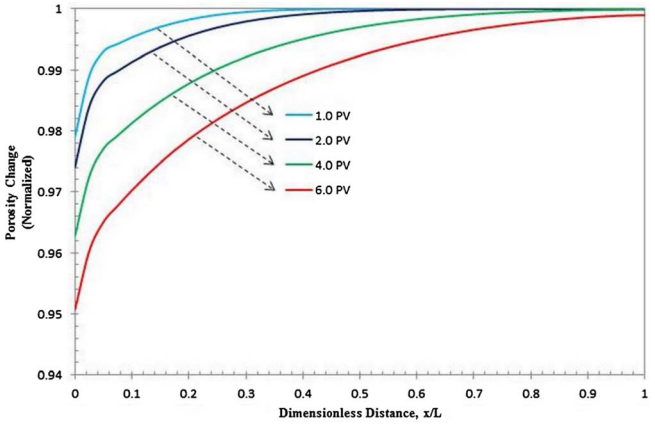

Fig. 16. Porosity profile at different injected PV.

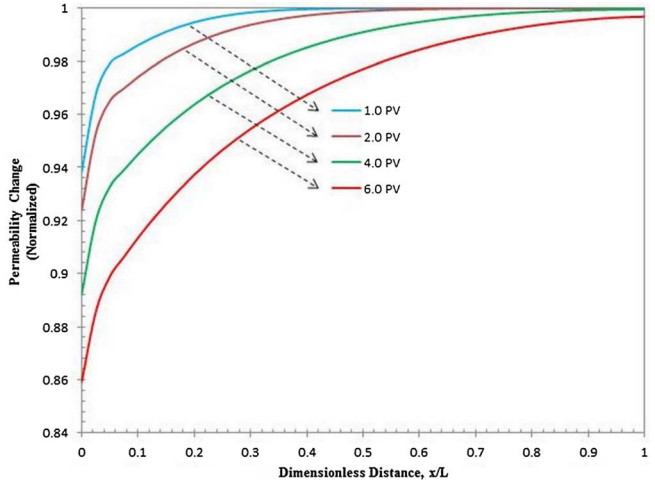

Fig. 17. Permeability profile at different injected PV.

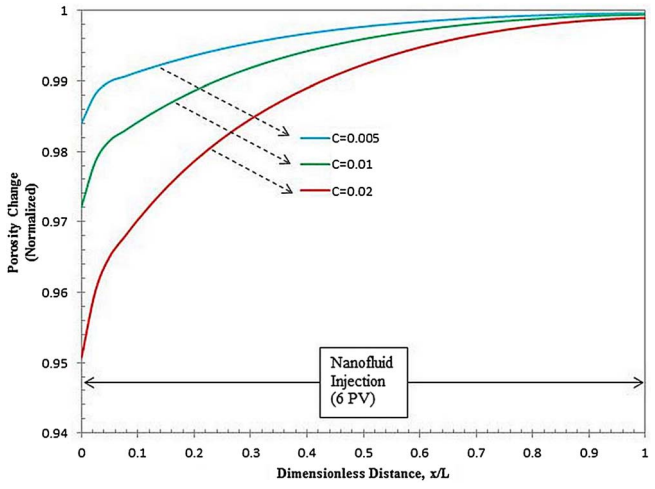

Fig. 18. Porosity profile at different inlet concentration.

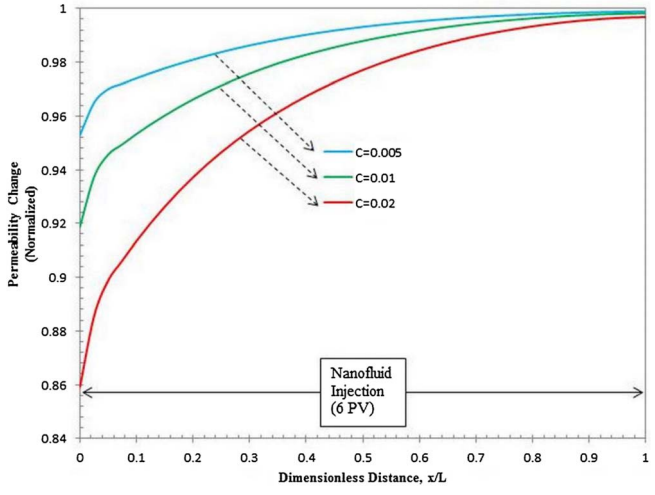

Fig. 19. Permeability profile at different inlet concentration.

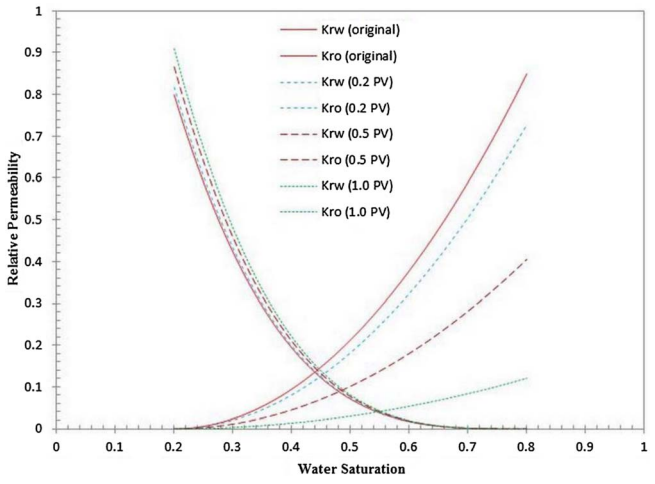

Fig. 20. Wettability alteration process for different injected PV of nanofluid (Cinlet = 0.02 cc/cc).

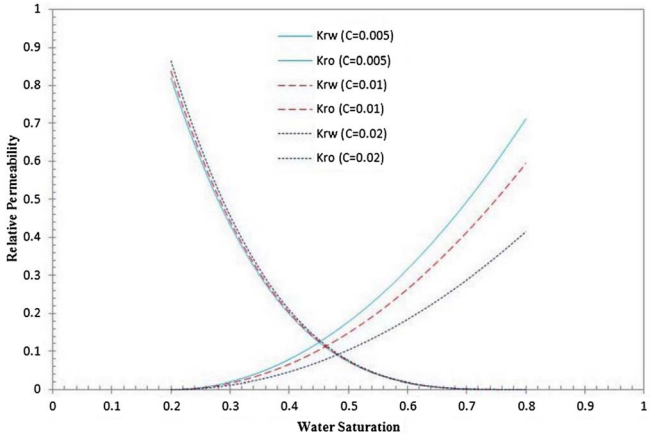

Fig. 21. Wettability alteration process for different inlet concentration (0.5 PV injected).

nanofluid, respectively. They show that increasing in injected PV or inlet concentration can lead to stronger wettability alteration. It should be noted that after injecting 1 PV of nanofluid with the concentration of 0.02 *cc/cc*, wettability alteration process is completely occurred.

Figure 22 shows the variation of net rate of loss of nanoparticles at the injection block (after 6 PV nanofluid injection at volume concentration of 0.02) due to nanoparticle adsorption on the pare walls and/or pore entrapment because of plugging or bridging. As can be seen, there are three stages of rate of nanoparticles' loss in porous media: raise, decline, and stability stages. According to nanoparticles adsorption and entrapment due to nanofluid injection, the raise stage can be described as the initial increasing of net rate of loss of nanoparticles from zero to a maximum peak. We believe that, for the decline stage, the difference of nanoparticles concentration between the current block and the next block (from inlet to outlet) can cause the nanoparticles diffusion from that block to the neighbor block which the previous block is a source of nanoparticles for the next block. Therefore, because of the diffusing of nanoparticles to the next block, the net rate of loss of nanoparticles in the previous block should be reduced to a minimum value. After the nanoparticles diffusion is relatively balanced through the core sample, net rate of loss of nanoparticles gradually and smoothly increases again due to less diffusion rate of nanoparticles for the desired block.

Figure 23 gives the profile of net rate of loss of nanoparticles for investigated core sample after 1 PV of nanofluid injection (at the concentration of 0.02). We can find out that the loss rate of nanoparticles from upstream to downstream reduces continuously. The higher rate of loss of nanoparticles for the upstream blocks can cause more intense wettability alteration and formation damage for these blocks, therefore fewer nanoparticles can pass through the core sample. Consequently, by reducing the concentration of nanoparticles along the core sample, the loss rate of nanoparticles must be reduced.

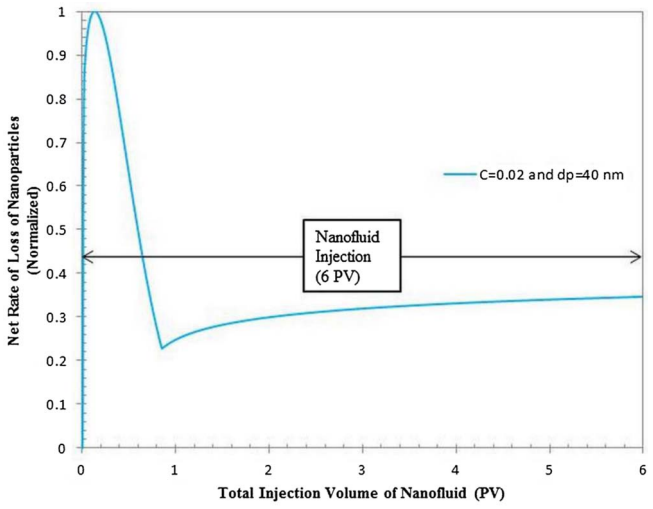

Fig. 22. Variation of net rate of loss of nanoparticles *versus* PV injected (during 6 PV nanofluid injection).

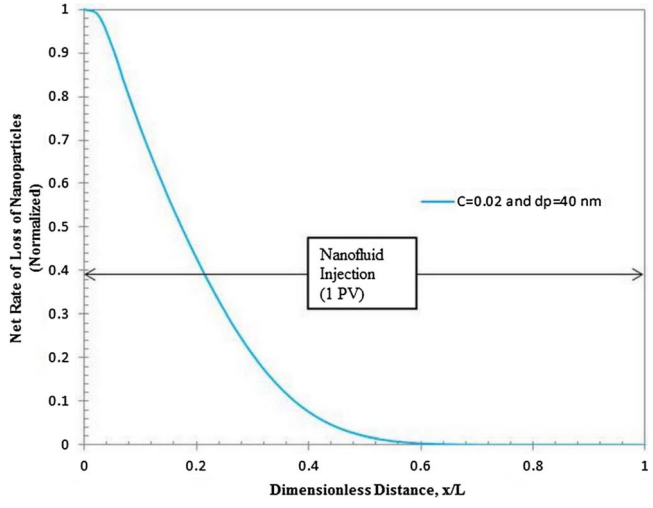

Fig. 23. The profile of net rate of loss of nanoparticles through core sample.

6 Conclusion

In the current study, we performed a set of experiments to investigate the effects of silica nanoparticles on the rock and fluid properties. Then, a numerical method was developed to model the experimental observations as well as predict the effects of silica nanoparticles on oil recovery and water cut. Based on the obtained results, conclusions are as follows:

1. The laboratory works show that the used nanoparticles' sizes are in the range of 20–70 nm, and a normal distribution is attributed to particles' size, approximately.
2. The experimental data shows that radii of the used carbonate samples' pores are about 8.0×10^0 to 5.2×10^4 nm.
3. The wettability of the carbonate rock surface could be changed from oil-wet to water-wet by using silica nanoparticles as well as oil-water interfacial tension reduction.
4. Higher concentration of the used silica nanoparticles can lead to higher oil recovery factor and the water cut can be reduced more intense and sooner.
5. The optimum concentration for the nanoparticles with sizes of 40 nm is at 2% vol. and the ultimate recovery can be improved 9.39% at this optimum condition; only 1 PV of nanofluid at optimum condition can complete the wettability alteration process.
6. With respect to sensitivity analysis on injection scenarios, the best injection scenario for high and low nanofluid concentrations are second and third, respectively.
7. Increasing in concentration and injection volume of the nanofluid can cause more intense formation damage (porosity and permeability reduction) particularly for injection region.
8. Increasing in concentration and injection volume of nanofluid can lead to more intense wettability alteration from oil-wet to water-wet.
9. Simulation results show that the net rate of loss of nanoparticles has three stages during nanofluid flooding: raise, decline, and stability; the profile of the loss rate of nanoparticles shows a decline behavior because of reducing nanoparticles' concentration along the investigated core sample.

Acknowledgments. The authors would like to thank Islamic Azad University, Science and Research Branch of Tehran (SRBIAU) and *National Iranian Oil Company (NIOC)* for their supports.

References

Abrams A., (1975) The influence of fluid viscosity, interfacial tension, and flow velocity on residual oil saturation left by waterflood, *SPE J.* **15**, 05, 437–447.

Ahmed T. (2006) *Reservoir engineering handbook*, Gulf Professional Publishing.

Al-Anssari S., Arif M., Wang S., Barifcani A., Lebedev M., Iglauer S. (2018) Wettability of nanofluid-modified oil-wet calcite at reservoir conditions *Fuel* **211**, 405–414.

Al-Anssari S., Barifcani A., Wang S., Maxim L., Iglauer S. (2016) Wettability alteration of oil-wet carbonate by silica nanofluid, *J Colloid Interface Sci.* **461**, 435–442.

Anderson W. (1986) Wettability literature survey-part 2: Wettability measurement, *J. Petrol. Technol.* **38**, 11, 1,246–1,62.

Archie G.E. (1952) Classification of carbonate reservoir rocks and petrophysical considerations, *AAPG Bull.* **36**, 2, 278–298.

Baez J., Ruiz M.P., Faria J., Harwell J.H., Shiau B., Resasco D.E. (eds) (2012) *Stabilization of interfacially-active-nanohybrids/polymer suspensions and transport through porous media*, Society of Petroleum Engineers.

Buckley J., Liu Y., Monsterleet S. (1998) Mechanisms of wetting alteration by crude oils, *SPE J.* **3**, 01, 54–61.

Cuiec L.E. (1990) Evaluation of reservoir wettability and its effect on oil recovery, in: Morrow N.R. (ed), *Interfacial phenomena in petroleum recovery*, Marcel Dekker, New York, pp. 319–370

El-Amin M.F., Salama A., Sun S. (eds) (2012) Modeling and simulation of nanoparticle transport in a two-phase flow in porous media, *SPE International Oilfield Nanotechnology Conference and Exhibition*, Society of Petroleum Engineers.

El-Amin M.F., Sun S., Salama A. (eds) (2013) Enhanced oil recovery by nanoparticles injection: modeling and simulation, *SPE Middle East Oil and Gas Show and Conference*, Society of Petroleum Engineers.

Ghosn R., Mihelic F., Hochepied J.F., Dalmazzone D. (2017) Silica nanoparticles for the stabilization of W/O emulsions at HTHP conditions for unconventional reserves drilling operations, *Oil Gas Sci. Technol. - Rev. IFP Energies nouvelles* **72**, 21.

Gruesbeck C., Collins R. (1982) Entrainment and deposition of fine particles in porous media, *SPE J.* **22**, 06, 847–856.

Hendraningrat L., Li S., Torsæter O. (2013) A coreflood investigation of nanofluid enhanced oil recovery, *J. Petrol. Sci. Eng.* **111**, 128–138.

Hendraningrat L., Shidong L. (eds) (2012) A glass micromodel experimental study of hydrophilic nanoparticles retention for EOR project, *SPE Russian Oil and Gas Exploration and Production Technical Conference and Exhibition*, Society of Petroleum Engineers.

Høgnesen E.J., Standnes D.C., Austad T. (2004) Scaling spontaneous imbibition of aqueous surfactant solution into preferential oil-wet carbonates, *Energy Fuels* **18**, 6, 1665–1675.

Ju B., Dai S., Luan Z., Zhu T., Su X., Qiu X. (eds) (2002) A study of wettability and permeability change caused by adsorption of nanometer structured polysilicon on the surface of porous media, *SPE Asia Pacific Oil and Gas Conference and Exhibition*, Society of Petroleum Engineers.

Ju B., Fan T., Li Z. (2012) Improving water injectivity and enhancing oil recovery by wettability control using nanopowders, *J. Petrol. Sci. Eng.* **86**, 206–216.

Ju B., Fan T., Ma M. (2006) Enhanced oil recovery by flooding with hydrophilic nanoparticles, *China Particuology* **4**, 01, 41–46.

Ju B., Fan T. (2009) Experimental study and mathematical model of nanoparticle transport in porous media, *Powder Technol.* **192**, 2, 195–202.

Kanj M.Y., Funk J.J., Al-Yousif Z. (eds) (2009) Nanofluid coreflood experiments in the ARAB-D, *SPE Saudi Arabia Section Technical Symposium*, Society of Petroleum Engineers.

Karimi A., Fakhroueian Z., Bahramian A., Pour Khiabani N., Babaee Darabad J., Azin R., Arya S. (2012) Wettability alteration in carbonates using zirconium oxide nanofluids: EOR implications, *Energy Fuels* **26**, 2, 1028–1036.

Kashefi S., Lotfollahi M.N., Shahrabadi A. (2018) Investigation of asphaltene adsorption onto zeolite beta nanoparticles to reduce asphaltene deposition in a silica sand pack, *Oil Gas Sci. Technol. - Rev. IFP Energies nouvelles* **73**, 2.

Løvoll G., Méheust Y., Måløy K.J., Aker E., Schmittbuhl J. (2005) Competition of gravity, capillary and viscous forces during drainage in a two-dimensional porous medium, a pore scale study, *Energy* **30**, 6, 861–872.

Maghzi A., Mohebbi A., Kharrat R., Ghazanfari M.H. (2011) Pore-scale monitoring of wettability alteration by silica nanoparticles during polymer flooding to heavy oil in a five-spot glass micromodel, *Transp. Porous Media* **87**, 3, 653–664.

Mandal A., Bera A., Ojha K., Kumar T. (eds) (2012) Characterization of surfactant stabilized nanoemulsion and its use in enhanced oil recovery, *SPE International Oilfield Nanotechnology Conference and Exhibition*, Society of Petroleum Engineers.

Metin C., Bonnecaze R., Nguyen Q. (2013) The viscosity of silica nanoparticle dispersions in permeable media, *SPE Reserv. Evalu. Eng.* **16**, 03, 327–332.

Miranda C.R., de Lara LS, Tonetto B.C. (eds) (2012) Stability and mobility of functionalized silica nanoparticles for enhanced oil recovery applications, *SPE International Oilfield Nanotechnology Conference and Exhibition*, Society of Petroleum Engineers.

Mohan K., Gupta R., Mohanty K. (2011) Wettability altering secondary oil recovery in carbonate rocks, *Energy Fuels* **25**, 9, 3966–3973.

Moradi B., Pourafshary P., Jalali F., Mohammadi M., Emadi M. (2015) Experimental study of water-based nanofluid alternating gas injection as a novel enhanced oil-recovery method in oil-wet carbonate reservoirs, *J. Nat. Gas Sci. Eng.* **27**, 64–73.

Moradi B., Pourafshary P., Jalali F., Mohammadi M. (2016) Effects of nanoparticles on gas production, viscosity reduction, and foam formation during nanofluid alternating gas injection in low and high permeable carbonate reservoirs, *Can. J. Chem. Eng.* **95**, 3, 479–490.

Morrow N.R. (1990) Wettability and its effect on oil recovery, *J. Petrol. Technol.* **42**, 12, 1476–1484.

North F.K. (1985) *Petroleum geology*, Allen & Unwin, Boston.

Ogolo N., Olafuyi O., Onyekonwu M. (eds) (2012) Enhanced oil recovery using nanoparticles, *SPE Saudi Arabia Section Technical Symposium and Exhibition*, Society of Petroleum Engineers.

Onyekonwu M.O., Ogolo N.A. (eds) (2010) *Investigating the use of nanoparticles in enhancing oil recovery*, Society of Petroleum Engineers.

Parvazdavani M., Masihi M., Ghazanfari M.H., Sherafati M., Mashayekhi L. (eds) (2012) *Investigation of the effect of water based nano-particles addition on hysteresis of oil-water relative permeability curves*, Society of Petroleum Engineers.

Puntervold T., Strand S., Austad T. (2007) Water flooding of carbonate reservoirs: Effects of a model base and natural crude oil bases on chalk wettability, *Energy Fuels* **21**, 3, 1606–1616.

Qin J., Li A. (2001) *Physics of oil reservoir*, China University of Petroleum Press, Dongying, pp. 151–152.

Qiu F., Mamora D.D. (eds) (2010) Experimental study of solvent-based emulsion injection to enhance heavy oil recovery in Alaska North slope area, *Canadian Unconventional Resources*, Society of Petroleum Engineers.

Romanovsky B., Makshina E. (2004) Nanocomposites as functional materials, *Soros Educational J.* **8**, 2.

Roustaei A., Bagherzadeh H. (2015) Experimental investigation of SiO_2 nanoparticles on enhanced oil recovery of carbonate reservoirs, *J. Petrol. Explor. Prod. Technol.* **5**, 1, 27–33.

Roustaei A., Moghadasi J., Bagherzadeh H., Shahrabadi A. (eds) (2012) *An experimental investigation of polysilicon nanoparticles*' recovery efficiencies through changes in interfacial tension and wettability alteration, Society of Petroleum Engineers.

Schlumberger Market Analysis (2007) Annual Report.

Sepehrinia K. (2017) Molecular dynamics simulation for surface and transport properties of fluorinated silica nanoparticles in water or decane: Application to gas recovery enhancement, *Oil Gas Sci. Technol. - Rev. IFP Energies nouvelles* **72**, 17.

Shahrabadi A., Bagherzadeh H., Roostaie A., Golghanddashti H. (eds) (2012) *Experimental investigation of HLP nanofluid*

potential to enhance oil recovery: A mechanistic approach, Society of Petroleum Engineers.

Skauge T., Spildo K., Skauge A. (eds) (2010) Nano-sized particles for EOR, *SPE Improved Oil Recovery Symposium*, Society of Petroleum Engineers.

Skjaeveland S., Siqveland L., Kjosavik A., Hammervold W., Virnovsky G. (eds) (1998) Capillary pressure correlation for mixed-wet reservoirs, *SPE India Oil*, Society of Petroleum Engineers.

Standnes D.C., Austad T. (2003) Wettability alteration in carbonates: Interaction between cationic surfactant and carboxylates as a key factor in wettability alteration from oil-wet to water-wet conditions, *Colloids Surf. A Physicochem. Eng. Aspects* **216**, 1, 243–259.

Standnes D.C., Austad T. (2000) Wettability alteration in chalk: 2. Mechanism for wettability alteration from oil-wet to water-wet using surfactants, *J. Petrol. Sci. Eng.* **28**, 3, 123–143.

Sun X., Zhang Y., Chen G., Gai Z. (2017) Application of nanoparticles in enhanced oil recovery: a critical review of recent progress, *Energies* **10**, 3, 345.

Tabrizy V.A., Hamouda A., Denoyel R. (2011) Influence of magnesium and sulfate ions on wettability alteration of calcite, quartz, and kaolinite: surface energy analysis, *Energy Fuels* **25**, 4, 1667–1680.

Vatanparast H., Alizadeh A., Bahramian A., Bazdar H. (2011) Wettability alteration of low-permeable carbonate reservoir rocks in presence of mixed ionic surfactants, *Petrol. Sci. Technol.* **29**, 18, 1873–1884.

Wagner O., Leach R.O. (1966) Effect of interfacial tension on displacement efficiency, *SPE J.* **6**, 04, 335–344.

Wang L., Zhang G., Li G., Zhang J., Ding B. (eds) (2010) *Preparation of microgel nanospheres and their application in EOR*, Society of Petroleum Engineers.

Yu J., An C., Mo D., Liu N., Lee R.L. (eds) (2012) Study of adsorption and transportation behavior of nanoparticles in three different porous media, *SPE Improved Oil Recovery Symposium*, Society of Petroleum Engineers.

Yu J., Berlin J.M., Lu W., Zhang L., Kan A.T., Zhang P., *et al.* (eds) (2010) *Transport study of nanoparticles for oilfield application*, Society of Petroleum Engineers.